Astron. Astrophys. 343, 650–660 (1999)

ASTRONOMY AND ASTROPHYSICS

Neutrino emission due to Cooper pairing of nucleons in cooling neutron stars

D.G. Yakovlev, A.D. Kaminker, and K.P. Levenfish

Ioffe Physical Technical Institute, Politekhnicheskaya 26, 194021 St.-Petersburg, Russia

Received 18 September 1998 / Accepted 29 October 1998

Abstract. The neutrino energy emission rate due to formation of Cooper pairs of neutrons and protons in the superfluid cores of neutron stars is studied. The cases of singlet-state pairing with isotropic superfluid gap and triplet-state pairing with anisotropic gap are analysed. The neutrino emission due to the singlet-state pairing of protons is found to be greatly suppressed with respect to the cases of singlet- or triplet-state pairings of neutrons. The neutrino emission due to pairing of neutrons is shown to be very important in the superfluid neutron–star cores with the standard neutrino luminosity and with the luminosity enhanced by the direct Urca process. It can greatly accelerate both, standard and enhanced, cooling of neutron stars with superfluid cores. This enables one to interpret the data on surface temperatures of six neutron stars, obtained by fitting the observed spectra with the hydrogen atmosphere models, by the standard cooling with moderate nucleon superfluidity.

Key words: dense matter – stars: neutron

1. Introduction

Neutron star interiors contain matter of nuclear and supranuclear density. Various microscopic theoretical models predict different compositions of this matter (neutrons, protons and electrons; hyperons; kaon or pion condensates; quarks), different equations of state (from very soft to very stiff) and superfluid properties of strongly interacting baryonic components (nucleons, hyperons, quarks).

Neutron stars are born very hot in supernova explosions but cool gradually in time. Their cooling depends on properties of stellar matter. Comparison of theoretical cooling models with observational data on the surface temperatures of isolated neutron stars yields a potentially powerful method to constrain models of superdense matter.

Young and middle-age ($t \lesssim 10^4$–10^5 yr) neutron stars cool mainly via neutrino emission from their interiors. It is important, thus, to know the main neutrino production mechanisms. For simplicity, we restrict ourselves by consideration of neutron stars whose cores are composed of neutrons (n), with some admixture of protons (p) and electrons (e). The neutrino emission mechanisms in the stellar cores may be divided into two groups, leading to *standard* or *rapid* cooling (e.g., Pethick 1992).

Send offprint requests to: D.G. Yakovlev (yak@astro.ioffe.rssi.ru)

The standard cooling lowers the surface temperature to about 10^6 K in $t \sim 10^4$ yr. It goes mainly via the modified Urca process (e.g., Friman & Maxwell 1979, Yakovlev & Levenfish 1995)

$$n + N \to p + N + e + \bar{\nu}_e, \;\; p + N + e \to n + N + \nu_e, \quad (1)$$

and the nucleon–nucleon bremsstrahlung

$$N + N \to N + N + \nu + \bar{\nu}, \quad (2)$$

where N is a nucleon (n or p).

Rapid cooling is strongly enhanced by the direct Urca reaction

$$n \to p + e + \bar{\nu}_e, \;\; p + e \to n + \nu_e, \quad (3)$$

which can operate (Lattimer et al. 1991) only in the central regions of rather massive neutron stars with not too soft equations of state. If the direct Urca reaction is allowed, the neutrino emissivity is typically 4–5 orders of magnitude higher than in the standard reactions (1) and (2), and the surface temperature decreases to several times of 10^5 K in $t \sim 10^4$ yr.

Cooling of neutron stars can be strongly affected by superfluidity of neutrons and protons in the stellar cores. The superfluidity is generally thought to be of BCS type produced under nuclear attraction of nucleons. At subnuclear densities $\rho \lesssim \rho_0$ (where $\rho_0 = 2.8 \times 10^{14}$ g cm^{-3} is the standard nuclear–matter density) the neutron pairing occurs due to nn attraction in the $^1S_0$ state. The superfluid gaps depend sensitively on nn interaction model. Various microscopic theories (e.g., Tamagaki 1970, Amundsen & Østgaard 1985, Baldo et al. 1992, Takatsuka & Tamagaki 1993, 1970) predict these gaps to vary in the range from some ten keV to some MeV. However, the singlet-state interaction of neutrons becomes repulsive at $\rho \sim \rho_0$, and, therefore, the singlet-state neutron superfluidity vanishes near the boundary between the neutron star core and the crust. Deeper in the core ($\rho \gtrsim \rho_0$), the triplet-state ($^3P_2$) nn interaction can be attractive to produce the superfluid with an anisotropic gap. Since the number density of protons is much smaller than that of neutrons, the singlet-state pp interaction is thought to be attractive in the stellar core leading to proton superfluidity. The superfluidity of n and p affects the main neutrino generation mechanisms

(1) – (3) in the neutron star cores, and hence cooling of neutron stars with superfluid interiors. Superfluidity always suppresses these reactions decreasing the neutrino luminosity of neutron stars.

However, the appearance of neutron or proton superfluid in a cooling neutron star initiates an additional specific neutrino production mechanism associated with the direct interband transition of a nucleon,

$$N \to N + \nu + \overline{\nu}. \tag{4}$$

The mechanism is allowed due to existence of a superfluid gap in the nucleon dispersion relation. The process may be called the neutrino emission due to *Cooper pair formation*. It was proposed and calculated for singlet-state neutron superfluidity by Flowers et al. (1976). It was rediscovered later by Voskresensky & Senatorov (1986, 1987). Until recently, the process has been 'forgotten', and has not been used in the studies of the neutron star cooling. It has been included into recent cooling simulations by Schaab et al. (1997), Page (1998), Yakovlev et al. (1998) and Levenfish et al. (1998) although its effect has not been analysed in details.

In Sect. 2 we present the derivation of the neutrino energy generation rate due to singlet and triplet Cooper pairing of nucleons. In the particular case of singlet–state nn pairing we reproduce the result by Flowers et al. (1976). The cases of triplet pairing of neutrons and singlet paring of protons appear to be different. In Sect. 3 we compare the Cooper-pair neutrino emission with other neutrino processes in the neutron star cores, and in Sect. 4 we analyse the effect of the Cooper-pair neutrinos on cooling of neutron stars with superfluid cores.

2. Cooper-pair neutrino emissivity

Consider neutrino emission due to Cooper pair formation (4) of nucleons. In the absence of superfluidity the process is strictly forbidden by energy–momentum conservation: a neutrino pair cannot be emitted by a free nucleon. Superfluidity introduces the energy gap into the nucleon dispersion relation near the Fermi surface which opens the reaction.

2.1. General formalism

Following Flowers et al. (1976) we will study the process (4) as annihilation $\tilde{N} + \tilde{N} \to \nu + \bar{\nu}$ of quasinucleons $\tilde{N}$ in a Fermi liquid with creation of a neutrino pair. The process goes via electroweak neutral currents; neutrinos of any flavors can be emitted. We will assume that nucleons are nonrelativistic and degenerate, and we will use the approximation of massless neutrinos. Let us derive the neutrino energy generation rate (emissivity) due to Cooper pairing of protons or neutrons in a triplet or singlet state. In this way we will generalize the results by Flowers et al. (1976) to the case of Cooper pairing of protons, and to the most important case of triplet pairing. The interaction Hamiltonian ($\hbar = c = 1$) is given by (e.g., Friman & Maxwell 1979)

$$H_w = -\frac{G_{\rm F}}{2\sqrt{2}} \left(c_V \, J_0 l_0 - c_A \, \boldsymbol{J} \cdot \boldsymbol{l} \right), \tag{5}$$

where $G_{\rm F}$ is the Fermi weak-interaction constant, and the terms containing c_V and c_A describe contributions of the vector and axial vector currents, respectively. The factors c_V and c_A are determined by quark composition of nucleons (e.g., Okun' 1990), and they are different for n and p. For the reactions with neutrons, one has $c_V = 1$ and $c_A = g_A$, while for those with protons, $c_V = 4 \sin^2 \Theta_{\rm W} - 1 \approx -0.08$ and $c_A = -g_A$, where $g_A \approx 1.26$ is the axial–vector constant and $\Theta_{\rm W}$ is the Weinberg angle ($\sin^2 \Theta_{\rm W} = 0.23$). Notice that similar interaction Hamiltonian describes the neutrino emission due to pairing of hyperons in neutron star matter. The latter process has been discussed in the literature (Balberg & Barnea 1998, Schaab et al. 1998) and will be considered briefly in Sect. 2.2.

Furthermore, in Eq. (5)

$$l^\mu = \overline{\psi}_\nu \gamma^\mu (1 + \gamma^5) \psi_\nu \tag{6}$$

is the neutrino 4-current (μ=0,1,2,3), γ^μ is a Dirac matrix, ψ_ν is a neutrino bispinor amplitude,

$$J_0 = \hat{\Psi}^+ \hat{\Psi}, \;\; \boldsymbol{J} = \hat{\Psi}^+ \boldsymbol{\sigma} \hat{\Psi} \tag{7}$$

is the nucleon 4-current and $\boldsymbol{\sigma}$ is the Pauli vector matrix.

The nucleon current contains $\hat{\Psi}$, the secondary-quantized nonrelativistic spinor wave function of quasi-nucleons in superfluid matter, and $\hat{\Psi}^+$, is its Hermitian conjugate. $\hat{\Psi}$ is determined by the Bogoliubov transformation. The transformation for singlet-state pairing is well known (e.g., Lifshitz & Pitaevskii 1980). The generalized Bogoliubov transformation for a triplet-state ^{3}P$_2$ pairing was studied in detail, for instance, by Tamagaki (1970). In the both cases $\hat{\Psi}$ can be written as

$$\hat{\Psi} \; = \; \sum_{\boldsymbol{p}\sigma\eta} \chi_\sigma \left[{\rm e}^{-iEt + i\boldsymbol{pr}} \, U_{\sigma\eta}(\boldsymbol{p}) \, \hat{\alpha}_{\boldsymbol{p}\eta} \right.$$
$$\left. + \;\; {\rm e}^{iEt - i\boldsymbol{pr}} \, V_{\sigma\eta}(-\boldsymbol{p}) \, \hat{\alpha}^+_{\boldsymbol{p}\eta} \right], \tag{8}$$

where $\boldsymbol{p}$ is a quasiparticle momentum,

$$E = \sqrt{\epsilon^2 + \Delta^2_{\boldsymbol{p}}} \tag{9}$$

is its energy with respect to the Fermi level (valid near the Fermi surface, at $|p - p_{\rm F}| \ll p_{\rm F}$), $\epsilon = v_{\rm F}(p - p_{\rm F})$, σ and $\eta = \pm 1$ enumerate spin states, $\Delta_{\boldsymbol{p}}$ is a superfluid gap at the Fermi surface ($\Delta_{\boldsymbol{p}} \ll p_{\rm F}\, v_{\rm F}$), $v_{\rm F}$ is the particle Fermi velocity; χ_σ is a basic spinor ($\chi^+_\sigma \chi_{\sigma'} = \delta_{\sigma\sigma'}$), $\hat{\alpha}_{\boldsymbol{p}\eta}$ and $\hat{\alpha}^+_{\boldsymbol{p}\eta}$ are, respectively, the annihilation and creation operators. $U_{\sigma\eta}(\boldsymbol{p})$ and $V_{\sigma\eta}(\boldsymbol{p})$ are matrix elements of the operators $U(\boldsymbol{p})$ and $V(\boldsymbol{p})$ which realize the Bogoliubov transformation from particle to quasiparticle states. In the cases of singlet and triplet pairing, one has

$$U_{\sigma\eta}(\boldsymbol{p}) = u_{\boldsymbol{p}}\, \delta_{\sigma\eta}, \;\; \sum_{\sigma\eta} |V_{\sigma\eta}(\boldsymbol{p})|^2 = 2\, v^2_{\boldsymbol{p}}, \tag{10}$$

where

$$u_{\boldsymbol{p}} = \sqrt{\frac{1}{2}\left(1 + \frac{\epsilon}{E}\right)}, \;\; v_{\boldsymbol{p}} = \sqrt{\frac{1}{2}\left(1 - \frac{\epsilon}{E}\right)}. \tag{11}$$

For a singlet-state pairing, the gap $\Delta_{\boldsymbol{p}}$ is actually independent of $\boldsymbol{p}$, so that $u_{\boldsymbol{p}}$ and $v_{\boldsymbol{p}}$ depend only on $p = |\boldsymbol{p}|$. For a triplet-state pairing, $\Delta_{\boldsymbol{p}}$, $u_{\boldsymbol{p}}$ and $v_{\boldsymbol{p}}$ depend on orientation of $\boldsymbol{p}$. Note general symmetry properties (e.g., Tamagaki 1970)

$$U_{\sigma\eta}(-\boldsymbol{p}) = U_{\sigma\eta}(\boldsymbol{p}), \;\; V_{\sigma\eta}(-\boldsymbol{p}) = -V_{\eta\sigma}(\boldsymbol{p}). \tag{12}$$

Let $q_\nu = (\omega_\nu, \boldsymbol{q}_\nu)$ and $q'_\nu = (\omega'_\nu, \boldsymbol{q}'_\nu)$ be 4-momenta of newly born neutrino and anti-neutrino, while $p = (E, \boldsymbol{p})$ and $p' = (E', \boldsymbol{p}')$ be 4-momenta of annihilating quasinucleons. Using the Fermi Golden rule one can easily obtain the neutrino emissivity in the form

$$Q \;=\; \left(\frac{G_\mathrm{F}}{2\sqrt{2}}\right)^2 \frac{1}{2}\mathcal{N}_\nu \int \frac{\mathrm{d}\boldsymbol{p}}{(2\pi)^3}\,\frac{\mathrm{d}\boldsymbol{p}'}{(2\pi)^3}\; f(E)f(E')$$
$$\times \int \frac{\mathrm{d}\boldsymbol{q}_\nu}{2\omega_\nu(2\pi)^3}\,\frac{\mathrm{d}\boldsymbol{q}'_\nu}{2\omega'_\nu(2\pi)^3}\;\left[c_V^2 I_{00}|l_0|^2 + c_A^2\, I_{ik} l_i l_k^*\right]$$
$$\times\; (2\pi)^4\,(\omega_\nu+\omega'_\nu)\,\delta^{(4)}(p+p'-q_\nu-q'_\nu)\,, \qquad (13)$$

where $\mathcal{N}_\nu$=3 is the number of neutrino flavors, an overall factor $1/2$ is introduced to avoid double counting of the same $\tilde{N}\tilde{N}$ collisions, integration is meant to be carried out over the domain $(q_\nu+q'_\nu)^2 > 0$ in which the process is kinematically allowed, $f(E) = 1/[\exp(E/T)+1]$ is the Fermi-Dirac distribution, T is the temperature, i,k=1,2,3, and

$$I_{00} \;=\; \sum_{\eta\eta'} |\langle B|\hat{\Psi}^+\hat{\Psi}|A\rangle|^2,$$
$$I_{ik} \;=\; \sum_{\eta\eta'} \langle B|\hat{\Psi}^+\sigma_i\hat{\Psi}|A\rangle\,\langle B|\hat{\Psi}^+\sigma_k\hat{\Psi}|A\rangle^*. \qquad (14)$$

In this case $|A\rangle$ denotes an initial state of the quasinucleon system (the individual states $(\boldsymbol{p},\eta)$ and $(\boldsymbol{p}',\eta')$ are occupied) and $|B\rangle$ is a final state of the system (the states $(\boldsymbol{p},\eta)$ and $(\boldsymbol{p}',\eta')$ are empty). In Eq. (13) we neglected the interference terms proportional to $c_V\,c_A$ since they vanish after subsequent integration over $\boldsymbol{p}$ and $\boldsymbol{p}'$.

Bilinear combinations of the neutrino current components (6) are calculated in the standard manner, and integration over $\mathrm{d}\boldsymbol{q}_\nu$ and $\mathrm{d}\boldsymbol{q}'_\nu$ is taken with the aid of the Lenard integral. The result is:

$$\int \frac{\mathrm{d}\boldsymbol{q}_\nu}{2\omega_\nu}\,\frac{\mathrm{d}\boldsymbol{q}'_\nu}{2\omega'_\nu}\; l^\alpha l^{\beta *}\,\delta^{(4)}(p+p'-q_\nu-q'_\nu)$$
$$= \frac{4\pi}{3}\;\left[q^\alpha q^\beta - (\omega^2-\boldsymbol{q}^2)\,g^{\alpha\beta}\right], \qquad (15)$$

where $q = (\omega, \boldsymbol{q})$ is 4-momentum of a neutrino pair ($\omega = \omega_\nu + \omega'_\nu = E+E'$, $\boldsymbol{q} = \boldsymbol{q}_\nu + \boldsymbol{q}'_\nu = \boldsymbol{p}+\boldsymbol{p}'$) and $g^{\alpha\beta}$ is the metric tensor. Inserting (15) into (13) we obtain

$$Q \;=\; \left(\frac{G_\mathrm{F}}{2\sqrt{2}}\right)^2 \frac{2\pi}{3}\,\frac{\mathcal{N}_\nu}{(2\pi)^8}\int \mathrm{d}\boldsymbol{p}\,\mathrm{d}\boldsymbol{p}'\; f(E)f(E')\,\omega$$
$$\times\;\left\{c_V^2\boldsymbol{q}^2 I_{00} + c_A^2\,\left[q_i q_k I_{ik} + (\omega^2-\boldsymbol{q}^2)\,I\right]\right\}, \qquad (16)$$

where $I = I_{xx}+I_{yy}+I_{zz}$.

Now the problem reduces to 6-fold integration over quasinucleon momenta $\boldsymbol{p}$ and $\boldsymbol{p}'$ within the kinematically allowed domain $\omega^2 > \boldsymbol{q}^2$. Since the nucleon Fermi liquid is assumed to be strongly degenerate, only narrow regions of momentum space near the nucleon Fermi-surface contribute into the reaction. Thus we can set $p = p_\mathrm{F}$ and $p' = p_\mathrm{F}$ in all smooth functions under the integral. One can prove that the presence of superfluidity (of energy gaps) makes the process kinematically allowed in a small region of momentum space where $\boldsymbol{p}$ is almost antiparallel to $\boldsymbol{p}'$. This allows us to set $\boldsymbol{p}' = -\boldsymbol{p}$ in all smooth functions in the integrand.

For further integration in Eq. (16) we write $\mathrm{d}\boldsymbol{p} = p_\mathrm{F}^2\,\mathrm{d}k\,\mathrm{d}\Omega$ and $\mathrm{d}\boldsymbol{p}' = p_\mathrm{F}^2\,\mathrm{d}k'\,\mathrm{d}\Omega'$, where $\mathrm{d}\Omega$ and $\mathrm{d}\Omega'$ are solid angle elements, $k = p - p_\mathrm{F}$ and $k' = p' - p_\mathrm{F}$. Let us integrate over $\mathrm{d}\Omega'$ first. For this purpose, we can fix $\boldsymbol{p}$ and introduce a local reference frame XYZ with the Z-axis antiparallel to $\boldsymbol{p}$. Let Θ and Φ be, respectively, azimuthal and polar angles of $\boldsymbol{p}'$ with respect to XYZ. Since the space allowed for $\boldsymbol{p}'$ is small, we have $\Theta \ll 1$, $q_X = q_\perp\cos\Phi$, $q_Y = q_\perp\sin\Phi$, $q_Z = k'-k \equiv q_\parallel$, where $q_\perp = p_\mathrm{F}\sin\Theta \approx p_\mathrm{F}\,\Theta$. In this case $\mathrm{d}\boldsymbol{p}' = \mathrm{d}k'\;q_\perp\,\mathrm{d}q_\perp\;\mathrm{d}\Phi$, $\boldsymbol{q}^2 = |\boldsymbol{p}+\boldsymbol{p}'|^2 = q_\parallel^2 + q_\perp^2$, and $\omega^2 - \boldsymbol{q}^2 = q_{\perp 0}^2 - q_\perp^2 \geq 0$, where $q_{\perp 0}^2 = \omega^2 - q_\parallel^2$. The quantities I_{00} and I_{ik} are smooth functions of $\boldsymbol{p}$ and $\boldsymbol{p}'$. In these functions, we set $\boldsymbol{p}' = -\boldsymbol{p}$ which makes them independent of $\boldsymbol{q}$. Therefore, q_X and q_Y are the only variables which depend on Φ. The integration over Φ in Eq. (16) contains the term,

$$\int_0^{2\pi} I_{ik}\,q_i q_k\,\mathrm{d}\Phi = \pi\left[2q_\parallel^2 I_{ZZ} + q_\perp^2\,(I_{XX}+I_{YY})\right]$$
$$= \pi\left[2q_\parallel^2 n_i n_k\,I_{ik} + q_\perp^2(\delta_{ik}-n_i n_k)\,I_{ik}\right], \qquad (17)$$

where $\boldsymbol{n} = \boldsymbol{p}/p$. Integration is performed in the local coordinate frame XYZ, but the result is transformed to the basic coordinate frame using tensor character of I_{ik}. Subsequent integration over $q_\perp$ from 0 to $q_{\perp 0}$ is easy and yields

$$Q \;=\; \left(\frac{G_\mathrm{F}}{2\sqrt{2}}\right)^2 \frac{\pi^2 p_\mathrm{F}^2}{6}\,\frac{\mathcal{N}_\nu}{(2\pi)^8}\int \mathrm{d}\Omega\;\int\!\!\int \mathrm{d}k\,\mathrm{d}k'\; f(E)f(E')$$
$$\times\;\omega\,(\omega^2-q_\parallel^2)\left\{2c_V^2(\omega^2+q_\parallel^2)I_{00}\right.$$
$$\left. +\;g_V^2\;\left[(5q_\parallel^2-\omega^2)\,I_{ik}n_i n_k + 3\,(\omega^2-q_\parallel^2)\,I\right]\right\}. \qquad (18)$$

Now we introduce dimensionless variables

$$x = \frac{v_\mathrm{F} k}{T},\;\; x' = \frac{v_\mathrm{F} k'}{T},\;\; z = \frac{E}{T},\;\; z' = \frac{E'}{T}, \qquad (19)$$

which give

$$Q \;=\; \left(\frac{G_\mathrm{F}}{2\sqrt{2}}\right)^2 \frac{\pi^2 p_\mathrm{F}^2}{6 v_\mathrm{F}^2}\,\frac{\mathcal{N}_\nu\,T^7}{(2\pi)^8}\int \mathrm{d}\Omega\;\int\!\!\int \mathrm{d}x\,\mathrm{d}x'$$
$$\times\;\frac{(z+z')}{(\mathrm{e}^z+1)(\mathrm{e}^{z'}+1)}\left[(z+z')^2 - \frac{(x-x')^2}{v_\mathrm{F}^2}\right]$$
$$\times\;\left\{2c_V^2\left[(z+z')^2 + \frac{(x-x')^2}{v_\mathrm{F}^2}\right]\;I_{00}\right.$$
$$+\;c_A^2\left[3\left((z+z')^2 - \frac{(x-x')^2}{v_\mathrm{F}^2}\right)\,I\right.$$
$$\left.\left.-\;\left((z+z')^2 - \frac{5\,(x-x')^2}{v_\mathrm{F}^2}\right)\,I_{ik}n_i n_k\right]\right\}, \qquad (20)$$

and the integration over x and x' is restricted by the domain where $(z+z') > |x-x'|/v_\mathrm{F}$. The outer integration is over orientations of nucleon momentum $\boldsymbol{p}$. Performing the inner integration over x and x' we can assume that this orientation is fixed (and the vector $\boldsymbol{n}$ is constant). Then the superfluid gap $\Delta_{\boldsymbol{p}}$

is fixed as well. Introducing $y = \Delta_{\boldsymbol{p}}/T$ we have $z = \sqrt{x^2 + y^2}$ and $z' = \sqrt{x'^2 + y^2}$. The integration domain can be rewritten as $(x - x')^2 - v_{\rm F}^2 (x + x')^2 \leq 4 v_{\rm F}^2 y^2/(1 - v_{\rm F}^2)$. In the nonrelativistic limit, we are interested in, $v_{\rm F} \ll 1$, and the domain transforms to the narrow strip in the xx' plane near the $x = x'$ line. It is sufficient to set $x' = x$ and $z' = z$ in smooth functions and integrate over $\delta x = x' - x$ in the narrow range $|\delta x| \leq 2 z v_{\rm F}$. In this way we come to a simple equation

$$\int_{-2zv_{\rm F}}^{2zv_{\rm F}} {\rm d}\delta x \left[(z+z')^2 - \frac{(x-x')^2}{v_{\rm F}^2} \right] \times \left\{ 2c_V^2 \left[(z+z')^2 + \frac{(x-x')^2}{v_{\rm F}^2} \right] I_{00} + c_A^2 \left[3 \left((z+z')^2 - \frac{(x-x')^2}{v_{\rm F}^2} \right) I - \left((z+z')^2 - \frac{5\,(x-x')^2}{v_{\rm F}^2} \right) I_{ik} n_i n_k \right] \right\} = \frac{2^9}{5} z^5 v_{\rm F} \, (c_V^2 I_{00} + c_A^2 I), \tag{21}$$

and the most sophisticated term containing $I_{ik} n_i n_k$ vanishes.

2.2. Practical formulae

Inserting (21) into (20) and returning to the standard physical units we have

$$Q = \frac{4 G_{\rm F}^2 m_N^* p_{\rm F}}{15 \pi^5 \hbar^{10} c^6} \, (k_{\rm B} T)^7 \, \mathcal{N}_\nu R = 1.170 \times 10^{21} \, \frac{m_N^*}{m_N} \, \frac{p_{\rm F}}{m_N c} \, T_9^7 \, \mathcal{N}_\nu \, R \;\; \frac{\rm erg}{\rm cm^3 \; s}, \tag{22}$$

where $m_N^* = p_{\rm F}/v_{\rm F}$ is an effective quasinucleon mass, m_N is bare nucleon mass, $T_9 = T/(10^9\,{\rm K})$, $k_{\rm B}$ is the Boltzmann constant, and

$$R = \frac{1}{8\pi} \int {\rm d}\Omega \int_0^\infty \frac{z^6 \, {\rm d}x}{({\rm e}^z + 1)^2} \, (c_V^2 \, I_{00} + c_A^2 \, I) \tag{23}$$

is a function to be determined. The integrand contains the functions I_{00} and $I = I_{xx} + I_{yy} + I_{zz}$ defined by Eqs. (14) with $\boldsymbol{p}' = -\boldsymbol{p}$ (see above). From Eqs. (10)–(12) for the singlet- and triplet-state pairings we obtain the same expression

$$I_{00} = 8 u_{\boldsymbol{p}}^2 v_{\boldsymbol{p}}^2 = 2 \frac{y^2}{z^2}. \tag{24}$$

In the case of the singlet-state pairing the Bogoliubov operator $V(\boldsymbol{p})$ possesses the properties $V_{\alpha\beta}(-\boldsymbol{p}) = V_{\alpha\beta}(\boldsymbol{p})$ and $V_{\alpha\beta}(\boldsymbol{p}) = -V_{\beta\alpha}(\boldsymbol{p})$, and has the form (e.g, Tamagaki 1970)

$$V_{\alpha\beta}(\boldsymbol{p}) = \begin{pmatrix} 0 & v_{\boldsymbol{p}} \\ -v_{\boldsymbol{p}} & 0 \end{pmatrix}. \tag{25}$$

Then from Eqs. (14) we have $I = 0$, i.e., the axial-vector contribution vanishes for the singlet-state pairing in accordance with the result by Flowers et al. (1976) (to be exact, the main term in the nonrelativistic expansion of Q over $(v_{\rm F}/c)^2$ vanishes). In this case the gap is isotropic and integration over dΩ is trivial:

$$R = c_V^2 F_s, \quad F_s = y^2 \int_0^\infty \frac{z^4 \, {\rm d}x}{({\rm e}^z + 1)^2}. \tag{26}$$

Table 1. Reaction constant a in Eq. (29)

particles	pairing	a
n, Ξ^0	^{1}S$_0$ (A)	1
n	^{3}P$_2$ (B,C)	$1 + 2g_A^2 = 4.17$
p, Ξ^-	^{1}S$_0$ (A)	$(1–4\sin^2\Theta_{\rm W})^2 = 0.0064$
p	^{3}P$_2$ (B,C)	$(1–4\sin^2\Theta_{\rm W})^2 + 2g_A^2 = 3.18$
$\Sigma^\pm$	^{1}S$_0$ (A)	$(2–4\sin^2\Theta_{\rm W})^2 = 1.17$
Λ, Σ^0	^{1}S$_0$ (A)	0

For the triplet-state pairing, according to Tamagaki (1970), $V_{\alpha\beta}(-\boldsymbol{p}) = -V_{\beta\alpha}(\boldsymbol{p})$, $V_{\alpha\beta}(\boldsymbol{p}) = V_{\beta\alpha}(\boldsymbol{p})$, and $V_{\alpha\beta}(\boldsymbol{p}) = v_{\boldsymbol{p}} \Gamma_{\alpha\beta}(\boldsymbol{p})$, where $\Gamma_{\alpha\beta}(\boldsymbol{p})$ is a unitary (2×2) matrix. Using these relationships and Eq. (10), for the triplet case from (14) we obtain

$$I = 8 u_{\boldsymbol{p}}^2 \sum_{\alpha\beta} |V_{\alpha\beta}(\boldsymbol{p})|^2 = 16 u_{\boldsymbol{p}}^2 v_{\boldsymbol{p}}^2 = 4 \, \frac{y^2}{z^2}, \tag{27}$$

which yields

$$R = (c_V^2 + 2\,c_A^2) \, F_t, \qquad F_t = \frac{1}{4\pi} \int {\rm d}\Omega \, y^2 \int_0^\infty \frac{z^4 \, {\rm d}x}{({\rm e}^z + 1)^2}. \tag{28}$$

Contrary to the singlet-state paring, the axial-vector contribution does not vanish.

The results (26) and (28) for ^{1}S$_0$ and ^{3}P$_2$ superfluids can be written in a unified manner:

$$R = a\,F, \tag{29}$$

where F stands for F_s or F_t, while $a = c_V^2$ or $c_V^2 + 2\,c_A^2$ is a dimensionless reaction constant that depends on the particle species and superfluid type. In Table 1 we list the values of a for singlet-state and triplet-state superfluids of neutrons and protons (calculated using the values of c_V and c_A cited in Sect. 2.1). (A) denotes ^{1}S$_0$ pairing, while (B) and (C) are two types of ^{3}P$_2$ pairing with total projection of the Cooper–pair momentum onto the z-axis equal to $m_J = 0$ and 2, respectively. One can hardly expect triplet-state pairing of protons in a neutron star core but we present the corresponding value for completeness of discussion. We give also the values of a for singlet-state pairing of hyperons. Hyperon superfluidity has been discussed recently by Balberg & Barnea (1998) and incorporated into calculations of the neutron star cooling by Schaab et al. (1998). The value of a for hyperons is determined by the vector constant c_V of weak neutral currents in Eq. (5) as a sum of contributions of corresponding quarks (e.g., Okun' 1990). One can see that the efficiency of the neutrino emission due to singlet-state pairing of various particles is drastically different. The emission is quite open for n, $\Sigma^\pm$, Ξ^0 but strongly (by two orders of magnitude) reduced for p and Ξ^-, and vanishes for Λ and Σ^0 hyperons. Notice that the values of c_V, c_A and a can be renormalized by manybody effects in dense matter which we ignore, for simplicity. Notice also that in the cases of singlet–state pairing of protons and Ξ^- the first non-vanishing relativistic corrections to the emissivity Q due to axial–vector neutral currents ($\sim v_{\rm F}^2$) could be larger than the small ($\sim c_V^2$) zero–order contribution of the vector currents. Since we neglect relativistic corrections, our expressions for Q in these cases may be somewhat inaccurate (give reliable lower limits of Q).

Eqs. (22) and (26) for singlet-state pairing of neutrons with two neutrino flavors ($\mathcal{N}_\nu = 2$) were obtained by Flowers et al. (1976). Similar equations were derived by Voskresensky & Senatorov (1986, 1987). Note that the final expressions for Q obtained by the latter authors contain a misprint: there is π^2 instead of π^5 in the denominator although the numerical formula includes the correct factor π^5. In addition, the expressions by Voskresensky & Senatorov (1986, 1987) are written for one neutrino flavor and erroneously contain the axial-vector contribution which is actually negligible.

Now we obtain practical expressions for the function F in Eq. (29). Following Levenfish & Yakovlev (1994a, b) we consider three types of BCS superfluid: (A), (B) and (C) as described above. In case (A) the superfluid gap is isotropic, $\Delta_A = \Delta_0^{(A)}(T)$. In cases (B) and (C) the gap is anisotropic and depends on angle θ between quasinucleon momentum $\boldsymbol{p}$ and the z-axis: $\Delta_B = \Delta_0^{(B)}(T)\sqrt{1+3\cos^2\theta}$, $\Delta_C = \Delta_0^{(C)}(T)\sin\theta$, respectively, where $\Delta_0(T)$ is a temperature-dependent amplitude. Therefore, at given T the gap Δ_B has minimum equal to $\Delta_0^{(B)}(T)$ for quasinucleons at the equator of the Fermi-sphere, whereas the gap Δ_C has maximum $\Delta_0^{(C)}(T)$ at the equator and nodes at the poles of the Fermi-sphere. In the cooling theories of neutron stars one commonly considers the nodeless pairing (B) of neutrons. However, thermodynamics of nucleon superfluid is very model-dependent and one cannot exclude that the C-type superfluid appears in the neutron star cores instead of the B-type, at least at some temperatures and densities.

Let us introduce the notations

$$v = \frac{\Delta_0(T)}{k_{\rm B}T}, \quad \tau = \frac{T}{T_c}, \tag{30}$$

where T_c is the critical temperature of nucleon superfluidity. Using the standard equations of the BCS theory, Levenfish & Yakovlev (1994a, b) obtained analytic fits which relate $\Delta_0(T)$ to τ at any $\tau < 1$ for all three superfluid types:

$$\begin{aligned} v_A &= \sqrt{1-\tau}\left(1.456 - \frac{0.157}{\sqrt{\tau}} + \frac{1.764}{\tau}\right), \\ v_B &= \sqrt{1-\tau}\left(0.7893 + \frac{1.188}{\tau}\right), \\ v_B &= \frac{\sqrt{1-\tau^4}}{\tau}\left(2.030\text{–}0.4903\,\tau^4 + 0.1727\,\tau^8\right). \end{aligned} \tag{31}$$

One can easily see that the function F in Eq. (29) depends actually on the only parameter v and on the superfluid type. An analysis of this function from Eqs. (26) and (28) is quite similar to that carried out by Levenfish & Yakovlev (1994b) in their study of the effect of superfluidity on the heat capacity of nucleons. Therefore we will omit technical details and present the final results.

Just after the superfluidity onset when the dimensionless gap parameter $v \ll 1$ and $\tau = T/T_c \to 1$, we obtain

$$\begin{aligned} F_A(v) &= 0.602\,v^2 = 5.65\,(1-\tau), \\ F_B(v) &= 1.204\,v^2 = 4.71\,(1-\tau), \\ F_C(v) &= 0.4013\,v^2 = 4.71\,(1-\tau). \end{aligned} \tag{32}$$

At temperatures T much below T_c one has $v \gg 1$ and

$$\begin{aligned} F_A(v) &= \frac{\sqrt{\pi}}{2}\,v^{13/2}\,{\rm e}^{-2v} = \frac{35.5}{\tau^{13/2}}\,{\rm e}^{-2v}, \\ F_B(v) &= \frac{\pi}{4\sqrt{3}}\,v^6\,{\rm e}^{-2v} = \frac{1.27}{\tau^6}\,{\rm e}^{-2v}, \\ F_C(v) &= \frac{50.03}{v^2} = 12.1\,\tau^2. \end{aligned} \tag{33}$$

Therefore the neutrino emission due to the nucleon pairing differs significantly from the majority of other neutrino reactions. The process has a threshold (becomes allowed at $T \le T_c$), and the neutrino emissivity Q is a nonmonotonic function of temperature. It grows rapidly with decreasing T just below T_c which does not happen in other reactions. With further decrease of T the emissivity Q reaches maximum and then decreases. According to Eqs. (33) the decrease of Q is exponential for the nodeless superfluids of (A) or (B), and it is power-law ($Q \propto T^9$) for the superfluid (C). The power-law behaviour of Q in case (C) occurs due to the presence of nodes in the superfluid gap. At $T \ll T_c$ superfluids (A), (B), and (C) suppress the Cooper-pair neutrino emission in the same manner in which they suppress the heat capacity and the direct Urca process (Levenfish & Yakovlev 1994a, b).

Finally, we have calculated $F(v)$ numerically in a wide range of v and fitted the results by simple expressions which reproduce also the asymptotes (32) and (33):

$$\begin{aligned} F_A(v) &= (0.602\,v^2 + 0.5942\,v^4 + 0.288\,v^6) \\ &\times \left(0.5547 + \sqrt{(0.4453)^2 + 0.01130\,v^2}\right)^{1/2} \\ &\times \exp\left(-\sqrt{4\,v^2 + (2.245)^2} + 2.245\right), \\ F_B(v) &= \frac{1.204\,v^2 + 3.733\,v^4 + 0.3191\,v^6}{1 + 0.3511\,v^2} \\ &\times \left(0.7591 + \sqrt{(0.2409)^2 + 0.3145\,v^2}\right)^2 \\ &\times \exp\left(-\sqrt{4\,v^2 + (0.4616)^2} + 0.4616\right), \\ F_C(v) &= (0.4013\,v^2 - 0.043\,v^4 + 0.002172\,v^6) \\ &\times (1\text{–}0.2018\,v^2 + 0.02601\,v^4 \\ &- 0.001477\,v^6 + 0.0000434\,v^8)^{-1}. \end{aligned} \tag{34}$$

The maximum fit error is about 1% at $v \approx 4$ for $F_A(v)$; about 3.4% at $v \approx 2$ for $F_B(v)$; and about 3% at $v \approx 1$ for $F_C(v)$.

3. Efficiency of Cooper-pair neutrinos

Eqs. (22), (29) and (34) enable one to calculate the neutrino emissivity Q due to Cooper pairing of nucleons or hyperons.

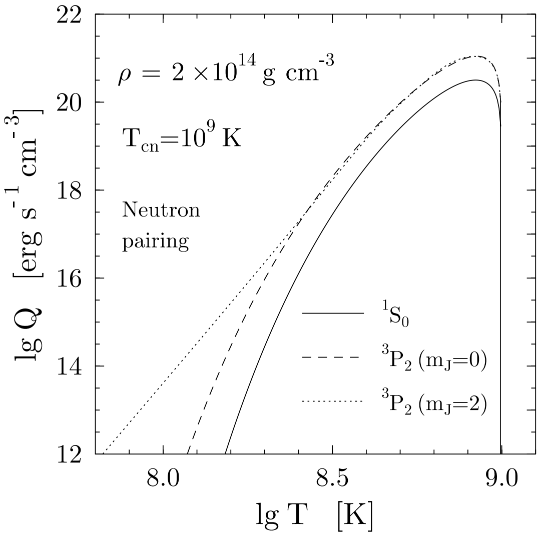

Fig. 1. Temperature dependence of the neutrino emissivity due to Cooper pairing of neutrons at $\rho = 2 \times 10^{14}$ g cm^{-3} and $T_{cn} = 10^9$ K for superfluidity (A) (solid line), (B) (dashed line) and (C) (dots).

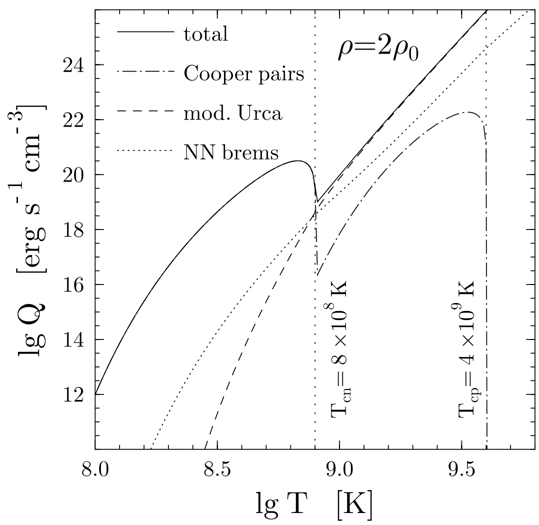

Fig. 2. Temperature dependence of the neutrino emissivities in different reactions at $\rho = 2\rho_0$ for neutron superfluid (B) with $T_{cn} = 8 \times 10^8$ K, and proton superfluid (A) with $T_{cp} = 4 \times 10^9$ K

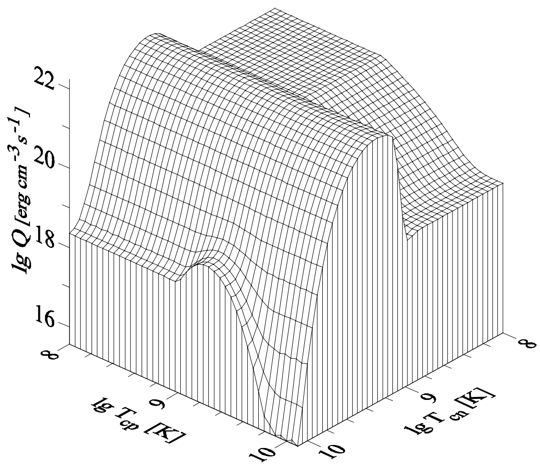

Fig. 3. Total neutrino emissivity versus T_{cn} and T_{cp} in a neutron star core at $\rho = 2\rho_0$ and $T = 10^9$ K.

For illustration, we use a moderately stiff equation of state in a neutron star core proposed by Prakash et al. (1988) (the version with the compression modulus $K_0 = 180$ MeV, and with the same simplified symmetry factor S_V that has been used by Page & Applegate, 1992). According to this equation of state, dense matter consists of neutrons with admixture of protons and electrons (no hyperons). We set the effective nucleon masses $m_N^* = 0.7\, m_N$, for simplicity. Since the critical temperatures T_{cn} and T_{cp} of the neutron and proton superfluids are model dependent (e.g., Tamagaki 1970, Amundsen & Østgaard 1985, Baldo et al. 1992, Takatsuka & Tamagaki 1993, 1970), we do not use any specific microscopic superfluid model but treat T_{cn} and T_{cp} as free parameters.

Fig. 1 shows temperature dependence of the emissivity Q produced by Cooper pairing of neutrons in the neutron star core at $\rho = 2 \times 10^{14}$ g cm^{-3}. The critical temperature is assumed to be $T_{cn} = 10^9$ K. Given ρ is typical for the transition from the singlet-state to the triplet-state pairing (Sect. 1). Thus various superfluid types are possible according to different microscopic theories. We present the curves for all three superfluid types (A), (B) and (C) discussed in Sect. 2.2. A growth of the emissivity with decreasing T below T_c is very steep. The main neutrino emission occurs in the temperature range $0.4\, T_c \lesssim T \lesssim T_c$. In this range, the emissivity depends weakly on the superfluid type and is rather high, of the order of or even higher than in the modified Urca reaction (1) in non–superfluid matter. This indicates that Cooper-pair neutrinos are important for neutron star cooling (Sect. 4).

Fig. 2 shows temperature dependence of various neutrino energy generation rates in a neutron star core at $\rho = 2\rho_0$. The neutron critical temperature is assumed to be $T_{cn} = 8 \times 10^8$ K, while the proton critical temperature is $T_{cp} = 4 \times 10^9$ K. We show the contributions from the modified Urca reaction (1) (sum of the proton and neutron branches), nucleon-nucleon bremsstrahlung (2) (sum of nn, np and pp contributions), Cooper pairing of nucleons (sum of n and p reactions), and also the total neutrino emissivity (solid line). The direct Urca process (3) is forbidden at given ρ. Here and in what follows the rates of the reactions (1)–(3) are taken as described in Levenfish & Yakovlev (1996), with proper account of suppression of the reactions by neutron and/or proton superfluidity (Levenfish & Yakovlev 1994a, Yakovlev & Levenfish 1995). The neutron superfluid is assumed to be of type (B) and the proton superfluid of type (A). A large bump of the total emissivity at $T \approx 10^{8.8}$ K is produced by the Cooper pairing of neutrons. If neutrino emission due to this pairing were absent the total neutrino emissivity at $T \lesssim T_{cn}$ would be 2–4 orders of magnitude smaller owing to the strong suppression by the nucleon superfluidity. The Cooper pairing can easily turn suppression into enhancement.

Fig. 3 shows a joint effect of the neutron and proton superfluids onto the total neutrino emissivity Q at $\rho = 2\rho_0$ and

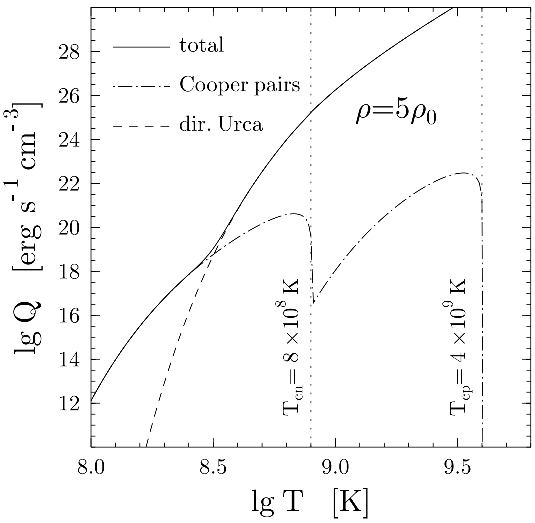

Fig. 4. Temperature dependence of the neutrino emissivities in main reactions at $\rho = 5\rho_0$ for neutron superfluid (B) with $T_{cn} = 8 \times 10^8$ K, and proton superfluid (A) with $T_{cp} = 4 \times 10^9$ K

$T = 10^9$ K. Presentation of Q as a function of T_{cn} and T_{cp} allows us to display all the effects of superfluidity onto the neutrino emission. If $T > T_{cn}$ and $T > T_{cp}$ we have Q in nonsuperfluid matter (a plateau at small T_{cn} and T_{cp}). For other T, the neutron and/or proton superfluidity affects the neutrino emission. It is seen that the neutron pairing at $T \lesssim T_{cn}$ may enhance the neutrino energy losses. A similar effect of the proton pairing at $T \lesssim T_{cp}$ is much weaker as explained above. In a strongly superfluid matter (highest T_{cn} and T_{cp}) the neutrino emission is drastically suppressed by the superfluidity.

Fig. 4 shows temperature dependence of some partial and total neutrino emissivities for the same T_{cn} and T_{cp} as in Fig. 2 but for higher density $\rho = 5\rho_0$. The equation of state we adopt opens the powerful direct Urca process at $\rho > \rho_{cr} = 1.30 \times 10^{15}$ g cm^{-3} $= 4.64\,\rho_0$. We take into account all major neutrino generation reactions (1)–(4). For simplicity, we do not show all partial emissivities since the total emissivity is mainly determined by the interplay between the direct Urca and Cooper pairing reactions.

The effect of Cooper-pair neutrinos is seen to be less important than for the standard neutrino reactions in Fig. 2 but, nevertheless quite noticeable. It is especially pronounced if $T \lesssim T_{cn} \ll T_{cp}$. In this case, the strong proton superfluid suppresses greatly the direct Urca process, and the emission due to Cooper pairing of neutrons can be significant.

Finally notice that while calculating neutron star cooling one often assumes the existence of one dominant neutrino generation mechanism, for instance, the direct Urca process for the enhanced cooling or the modified Urca process for the standard cooling. This is certainly true for non–superfluid neutron–star cores, but wrong in superfluid matter. In the latter case, different mechanisms can dominate (Fig. 5) at various cooling stages depending on temperature, T_{cn}, T_{cp}, and density.

In particular, the Cooper-pair neutrinos dominate the standard neutrino energy losses at $T \lesssim 10^9$ K for a moderate neutron superfluidity ($0.12 \lesssim T/T_{cn} \lesssim 0.96$). This parameter range is important for cooling theories. At the early cooling stages, when $T \gtrsim 10^9$ K, the Cooper-pair neutrinos can also be important but in a narrower range around $T/T_{cn} \approx 0.4$ especially in the presence of the proton superfluid. As mentioned above, Cooper-pair neutrinos can dominate also in the regime of rapid neutrino emission if the nucleons of one species are strongly superfluid but the other nucleons are moderately or weakly superfluid (see Fig. 5b).

Figs. 5a and b display the domains of T_{cn} and T_{cp}, where different neutrino mechanisms are dominant. Fig. 5a refers to the standard cooling at $\rho = 2\,\rho_0$ and $T = 3 \times 10^8$ K. Fig. 5b corresponds to the rapid cooling at $\rho = 5\,\rho_0$ and $T = 10^8$ K. Dashes show the lines of $T = T_{cn}$ and $T = T_{cp}$, which separate T_{cn}-T_{cp} planes into four regions. In the left down corners enclosed by these lines, matter is nonsuperfluid. The right down corners correspond to superfluidity of n alone; the left upper corners to superfluidity of p alone, and the right upper corners to joint n and p superfluidity. One can observe a variety of dominant cooling mechanisms regulated by the superfluidity. If both n and p superfluids are very strong, they switch off all the neutrino emission mechanisms involving nucleons (and discussed here). In this regime, a slow neutrino emission due to ee–bremsstrahlung (Kaminker et al. 1997) survives and dominates. This mechanism is rather insensitive to the superfluid state of dense matter.

4. Models of cooling neutron stars

To illustrate the results of Sects. 2 and 3 we have performed simulations of neutron–star cooling. We have used the same cooling code as described by Levenfish & Yakovlev (1996). The general relativistic effects are included explicitly. The stellar cores are assumed to have the same equation of state (Prakash et al., 1988) as has been used in Sect. 3. The maximum neutron–star mass, for this equation of state, is $1.73\,M_\odot$. We consider the stellar models with two masses. In the first case, the mass is $M = 1.3\,M_\odot$, the radius $R = 11.87$ km, and the central density $\rho_c = 1.07 \times 10^{15}$ g cm^{-3} is below the threshold (ρ_{cr}) of the direct Urca process; this is an example of the standard cooling. In the second case $M = 1.48\,M_\odot$, $R = 11.44$ km, and $\rho_c = 1.376 \times 10^{15}$ g cm^{-3}. The powerful direct Urca process is open in a small central stellar kernel of radius 2.32 km and mass $0.035\,M_\odot$, producing enhanced cooling. Notice, that in calculations of the equation of state of the stellar core in our earlier articles (Levenfish & Yakovlev 1996, and references therein) the parameter n_0 (standard saturation number density of baryons) was set equal to 0.165 fm^{-3}. In the present article, we adopt a more natural choice $n_0 = 0.16$ fm^{-3} and use the model of the rapidly cooling star with somewhat higher mass than before ($1.44\,M_\odot$). The nucleon effective masses are set equal to 0.7 of their bare masses.

For simplicity, the nucleons are assumed to be superfluid everywhere in the stellar core. We suppose that the proton superfluidity is of type (A), while the neutron superfluidity is of type (B). We make the simplified assumption that T_{cn} and T_{cp}

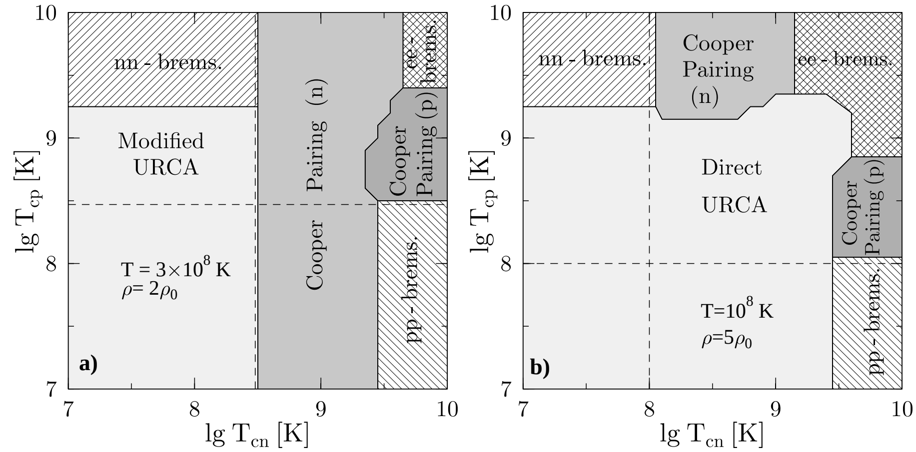

Fig. 5a and b. Domains of T_{cp} and T_{cn}, where different neutrino emission mechanisms dominate (different shaded regions). In addition to the mechanisms (1)–(4) we include also the neutrino emission due to ee bremsstrahlung (Kaminker et al. 1997). **a** corresponds to the standard neutrino emission at $\rho = 2\,\rho_0$ and $T = 3 \times 10^8$ K, while **b** refers to the emission enhanced by the direct Urca process at $\rho = 5\,\rho_0$ and $T = 10^8$ K. Dashed lines correspond to $T_{cn} = T$ or $T_{cp} = T$.

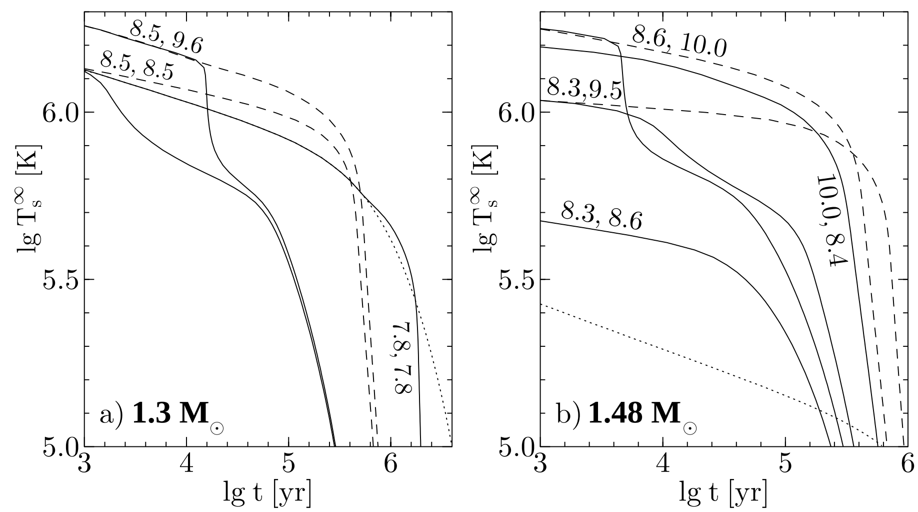

Fig. 6a and b. Redshifted surface temperature T_s^∞ versus age t for the standard **a** and enhanced **b** cooling of the 1.3 $M_\odot$ and 1.48 $M_\odot$ neutron stars, respectively. Dotted curves are for non–superfluid stars. Solid and dashed curves are for superfluid stars (marked with ($\lg T_{cn}, \lg T_{cp}$)) including and neglecting Cooper-pair neutrinos, respectively. Solid and dashed curves (7.8,7.8) in **a**, and (8.3,8.6) and (10,8.4) in **b** coincide.

are constant over the stellar core and can be treated as free parameters (see Sect. 3).

Our cooling code includes the main traditional neutrino reactions in the neutron star core (1)–(3), suppressed properly by neutron and proton superfluids (Levenfish & Yakovlev 1996), supplemented by the Cooper neutrino emission by neutrons and protons (Sects. 2 and 3). In addition we include the neutrino emission due to electron-ion bremsstrahlung in the neutron star crust using an approximate formula by Maxwell (1979). The neutron–star heat capacity is assumed to be the sum of the capacities of n, p, and e in the stellar core affected by n and p superfluids (Levenfish & Yakovlev 1994b). We have neglected the heat capacity of the crust due to small crustal masses for the chosen stellar models. Our cooling code is based on approximation of isothermal stellar interior valid for a star of age $t > (10–10^3)$ yr, inside which the thermal relaxation is over. We use the relationship between the surface and interior stellar temperature obtained by Potekhin et al. (1997). We assume that the stellar atmosphere may contain light elements. Then we can compare our results with observations of thermal radiation interpreted using the hydrogen or helium atmosphere models. However the mass of light elements is postulated to be insufficient ($\lesssim 10^{-14} M_\odot$) to affect the cooling.

Figs. 6a and b show typical cooling curves (dependence of the effective surface temperature T_s^∞ versus stellar age t) for the neutron stars with superfluid cores. The effective temperature is redshifted (as detected by a distant observer). Fig. 6a displays the standard cooling, while 6b shows the enhanced cooling. It is seen that Cooper-pair neutrino emission can be either important or unimportant for the cooling of both types depending on T_{cn}, T_{cp} and t. Its effect is to accelerate the cooling, and the stronger effect takes place if the neutron or proton superfluidity is switched on in the neutrino cooling era ($t \lesssim 10^5$ yr). As mentioned in Sect. 3, the neutrinos provided by neutron pairing can dominate the neutrino emission from the modified Urca process at temperatures $T \lesssim T_{cn} \lesssim 10^9$ K. Therefore, if the neutron superfluidity with $T_{cn} \lesssim 10^9$ K is switched on in the stellar core, the standard cooling is accelerated. The acceleration is especially dramatic if the modified Urca was suppressed by the proton superfluidity before the onset of the neutron superfluidity ($T_{cn} \ll T_{cp}$). Then the slow cooling looks like the enhanced one (cf Figs. 6a and b). On the other hand, Cooper-pair neutrinos can be unimportant. The example is given by the curve ($\lg T_{cn} = 7.8$, $\lg T_{cp} = 7.8$) in Fig. 6a. In this case, the star enters the photon cooling era (with the photon surface luminosity much larger than the neutrino one) with the internal

Table 2. Observational data

Source	$\lg t$, [yr]	Atmosphere model[b]	$\lg T_s^\infty$, [K]	Confidence level[a]	Reference
RX J0822-43	3.57	Hydrogen atmosphere	$6.23^{+0.02}_{-0.02}$	95.5%	Zavlin et al. (1998b)
		Black body	$6.61^{+0.05}_{-0.05}$	95.5%	Zavlin et al. (1998b)
1E 1207-52	3.85	Hydrogen atmosphere	$6.10^{+0.05}_{-0.06}$	90%	Zavlin et al. (1998a)
		Black body	$6.49^{+0.02}_{-0.01}$	90%	Zavlin et al. (1998a)
RX J0002+62	3.95[c]	Hydrogen atmosphere	$6.03^{+0.03}_{-0.03}$	95.5%	Zavlin et al. (1998b)
		Black body	$6.18^{+0.18}_{-0.18}$	95.5%	Zavlin et al. (1998b)
PSR 0833-45 (Vela)	4.4[d]	Hydrogen atmosphere	$5.90^{+0.04}_{-0.01}$	90%	Page et al. (1996)
		Black body	$6.24^{+0.03}_{-0.03}$	—	Ögelman (1995)
PSR 0656+14	5.00	Hydrogen atmosphere	$5.72^{+0.04}_{-0.02}$	—	Anderson et al. (1993)
		Black body	$5.96^{+0.02}_{-0.03}$	90%	Possenti et al. (1996)
PSR 0630+178 (Geminga)	5.53	Hydrogen atmosphere	$5.25^{+0.08}_{-0.01}$	90%	Meyer et al. (1994)
		Black body	$5.75^{+0.05}_{-0.08}$	90%	Halpern, Wang (1997)
PSR 1055-52	5.73	Black body	$5.88^{+0.03}_{-0.04}$	—	Ögelman (1995)

[a] Confidence level of T_s^∞ (90% and 95.5% correspond to 1.64σ and 2σ, respectively); dash means that the level is not indicated in cited references.
[b] Method for interpretation of observation.
[c] The mean age taken according to Craig et al. (1997).
[d] According to Lyne et al. (1996).

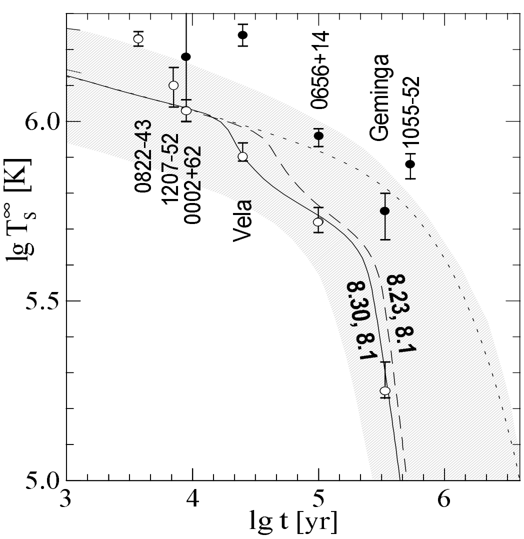

Fig. 7. Standard cooling curves (1.3 $M_\odot$) compared with observations (Table 2). Error bars are 90%–95% estimates of T_s^∞ obtained by fitting the observed radiation spectra with black-body spectrum (filled circles) and atmosphere models (open circles). Dotted curve corresponds to a non-superfluid star. Solid and dashed curves labelled as in Fig. 6 are for superlfuid stars. Dashed region is formed by standard the curves for different T_{cn} and T_{cp}.

temperature $T \lesssim 10^8$ K. The superfluidity appears later, and has naturally almost no effect on the cooling. If $T_{cn} \ll T_{cp}$ the Cooper neutrino emission by neutrons can dominate even the powerful direct Urca process and accelerate the enhanced cooling (Fig. 6b). In other cases (e.g., the curves ($\lg T_{cn} = 8.3$, $\lg T_{cp} = 8.6$) and ($\lg T_{cn} = 10$, $\lg T_{cp} = 8.4$)) the effect of Cooper–pair neutrinos on the enhanced cooling can be unimportant.

Fig. 7 compares the standard cooling curves (1.3 $M_\odot$) with the available observations of thermal radiation from isolated neutron stars. The observational data are summarized in Table 2. We include the data on four pulsars (Vela, Geminga, PSR 0656+14, PSR 1055-52) and three radioquiet objects (RX J0822-43, 1E 1207-52, RX J0002+62) in supernova remnants. The pulsar ages are the dynamical ages except for Vela, where new timing results by Lyne et al. (1996) are used. Ages of radioquiet objects are associated to ages of their supernova remnants. The error bars give the confidence intervals of the redshifted effective surface temperatures obtained by two different methods. The first method consists in fitting the observed spectra by neutron–star hydrogen and/or helium atmosphere models (open circles), and the second one consists in fitting by the blackbody spectrum (filled circles). Dashed region encloses all standard cooling curves for a 1.30 $M_\odot$ star with different T_{cn} and T_{cp} (from 10^6 K to 10^{10} K). Notice that the Cooper-pair neutrinos introduce into the cooling theory some new "degree of freedom" which helps one to fit the observational data. For instance, we present a solid curve which hits five error bars for the atmosphere models at once. We would not be able to find a similar cooling curve if we neglected the Cooper-pair neutrino emission. The dashed curve in Fig. 7 shows that Cooper-pair neutrinos make the standard cooling very sensitive to the superfluid parameters. A minor change even of the one superfluid parameter yields quite a different cooling curve, which hits two error bars only. Such a sensitivity is important for constraining T_{cn} and T_{cp} from observations.

Thus, the majority of observations of thermal radiation from isolated neutron stars can be interpreted by the standard cooling with quite a moderate nucleon superfluidity in the stellar core. These moderate critical temperatures do not contradict to a wealth of microscopic calculations of T_{cp} and T_{cn}. Notice that it is easier for us to explain the "atmospheric" surface temperatures than the blackbody ones. This statement can be considered as an indirect argument in favour of the atmospheric interpretation of the thermal radiation. Although the theory of neutron–star atmospheres is not yet complete (e.g., Pavlov & Zavlin 1998) the atmospheric fits give more reasonable neutron–star parameters (radii, magnetic fields, distances, etc.) which are in better agreement with the parameters obtained by other independent methods.

Even in our simplified model (one equation of state, two fixed neutron–star masses, constant T_{cn} and T_{cp} over the stellar core) it is possible to choose quite definite superfluid parameters to explain most of observations. However, one needs more elaborated models of cooling neutron stars to obtain reliable information on superfluid state of the neutron star cores. We expect to develop such models in the future making use of the results obtained in the present article.

5. Conclusions

We have reconsidered the neutrino emission rate due to Cooper pairing of nucleons in the neutron star cores (Sect. 2). We have presented the results in the form convenient for practical implications in three cases: (A) singlet–state $^1S_0$ pairing, (B) triplet–state $^3P_2$ pairing with zero projection of the Cooper pair momentum ($m_J = 0$) onto quantization axis, and (C) triplet–state pairing with maximum ($m_J = 2$) momentum projection. For the singlet-state pairing of neutrons, our results agree with those by Flowers et al. (1976). For the triplet-state pairing our consideration is original. Notice an essential difference of the Cooper-pair neutrino emissivities for singlet and triplet-state superfluids and also for neutrons and protons. In Sect. 3 we have analysed the efficiency of the Cooper-pair neutrino emission at different densities in the neutron star cores as compared with the traditional neutrino production mechanisms including a powerful direct Urca process allowed at high densities. Contrary to the non-superfluid cores where the main neutrino emission is produced either by the modified or by the direct Urca processes (depending on equation of state and density), very different neutrino mechanisms can dominate in the superfluid cores at certain temperatures T and superfluid critical temperatures T_{cn} and T_{cp}. In particular, neutrinos produced by pairing of neutrons can be very important if $T \lesssim T_{cn} \ll T_{cp}$. The importance of these neutrinos in the standard and rapid cooling of the neutron stars has been analysed in Sect. 4. We show that, under certain conditions, neutrinos provided by pairing of neutrons can greatly accelerate both standard and enhanced cooling of middle-age neutron stars (t= 10^4–10^5 yr). In particular, the accelerated standard cooling can mimic rapid cooling of the stars. The Cooper-pair neutrinos modify the cooling curves and enable us to explain observations of thermal radiation of several neutron stars by one cooling curve at once. This confirms the potential ability (Page & Applegate, 1992) to constrain the fundamental parameters of superdense matter in the neutron star cores, the critical temperatures of neutron and proton superfluids, by comparing theory and observation of neutron stars.

Acknowledgements. We are grateful to D.A. Baiko, P. Haensel, C.J. Pethick, Yu.A. Shibanov, D.A. Varshalovich and D.N. Voskresensky for useful discussions. This work was supported in part by RFBR (grant 96-02-16870a), RFBR-DFG (grant 96-02-00177G) and INTAS (grant 96-0542).

References

Amundsen L., Østgaard E., 1985, Nucl. Phys. A442, 163
Anderson S., Córdova F., Pavlov G.G., Robinson C.R., Thompson R.J., 1993, ApJ 414, 867
Balberg S., Barnea N., 1998, Phys. Rev. 57C, 409
Baldo M., Cugnon J., Lejeune A., Lombardo U., 1992, Nucl. Phys. A536, 349
Craig W.W., Hailey Ch.J., Pisarski R.L., 1997, ApJ 488, 307
Flowers E., Ruderman M., Sutherland P., 1976, ApJ 205, 541
Friman B.L., Maxwell O.V., 1979, ApJ 232, 541
Halpern J., Wang F., 1997, ApJ 477, 905
Kaminker A.D., Yakovlev D.G., Haensel P., 1997, A&A 325, 391
Lattimer J.M., Prakash M., Pethick C.J., Haensel P., 1991, Phys. Rev. Lett. 66, 2701
Levenfish K.P., Yakovlev D.G., 1994a, Astron. Lett. 20, 43
Levenfish K.P., Yakovlev D.G., 1994b, Astron. Rep. 38, 247
Levenfish K.P., Yakovlev D.G., 1996, Astron. Lett. 22, 47
Levenfish K.P., Shibanov Yu.A., Yakovlev D.G., 1998, Physica Scripta T77, 79
Lifshitz E.M., Pitaevskii L.P., 1980, Statistical Physics. Part 2, Pergamon, Oxford
Lyne A.G., Pritchard R.S., Graham-Smith F., Camilo F., 1996, Nat 381, 497
Maxwell O.V., 1979, ApJ 231, 201
Meyer R.D., Pavlov G.G., Mészàros P., 1994, ApJ 433, 265
Ögelman H., 1995, In: Alpar M.A., Kiziloğlu Ü, van Paradijs J. (eds.) Lives of Neutron Stars. Kluwer Academic Publishers, Dordrecht, p. 101
Okun' L.B., 1990, Leptons and Quarks. Nauka, Moscow (in Russian)
Page D., 1998, In: Buccheri R., van Paradijs J., Alpar M.A. (eds.) The Many Faces of Neutron Stars. Kluwer, Dordrecht, p. 538
Page D., Applegate J.H., 1992, ApJ 394, L17
Page D., Shibanov Yu., Zavlin V., 1996, In: Zimmermann H.U., Trümper J.E., Yorke H. (eds.) Röntgenstrahlung from the Universe. MPE, Garching, p. 173
Pavlov G.G., Zavlin V.E., 1998, In: Shibazaki N., Kawai N., Shibata S., Kifune T. (eds.) Neutron Stars and Pulsars. Universal Academy Press, Tokyo, p. 327
Pethick C.J., 1992, Rev. Mod. Phys. 64, 1133
Potekhin A.Yu., Chabrier G., Yakovlev D.G., 1997, A&A 323, 415
Prakash M., Ainsworth T.L., Lattimer J.M., 1988, Phys. Rev. Lett. 61, 2518
Possenti A., Mereghetti S., Colpi M., 1996, A&A 313, 565
Schaab Ch., Voskresensky D., Sedrakian A.D., Weber F., Weigel M.K., 1997, A&A 321, 591

Schaab Ch., Balberg S., Schaffner-Bielich J., 1998, ApJL 504, L99
Takatsuka T., Tamagaki R., 1993, Prog. Theor. Phys. Suppl. 112, 27
Takatsuka T., Tamagaki R., 1997, Prog. Theor. Phys. 97, 345
Tamagaki R., 1970, Prog. Theor. Phys. 44, 905
Voskresensky D., Senatorov A., 1986, Sov. Phys.–JETP 63, 885
Voskresensky D., Senatorov A., 1987, Sov. J. Nucl. Phys. 45, 411
Yakovlev D.G., Levenfish K.P., 1995, A&A 297, 717
Yakovlev D.G., Kaminker A.D., Levenfish K.P., 1998, In: Shibazaki N., Kawai N., Shibata S., Kifune T. (eds.) Neutron Stars and Pulsars. Universal Academy Press, Tokyo, p. 195
Zavlin V., Pavlov G.G., Trümper J., 1998a, A&A 331, 821
Zavlin V., Pavlov G.G., Trümper J., 1998b, X–ray emission from neutron stars in two supernova remnants. A&A (accepted)